European Journal of Radiology 117 (2019) 33–40

Contents lists available at ScienceDirect

European Journal of Radiology

journal homepage: www.elsevier.com/locate/ejrad

Radiomics analysis enables recurrence prediction for hepatocellular carcinoma after liver transplantation

Donghui Guo[a,1], Dongsheng Gu[c,1], Honghai Wang[b], Jingwei Wei[c], Zhenglu Wang[b], Xiaohan Hao[c], Qian Ji[b], Shunqi Cao[a], Zhuolun Song[b], Jiabing Jiang[a], Zhongyang Shen[b], Jie Tian[c,**], Hong Zheng[b,*]

[a] First Central Clinical College of Tianjin Medical University, Tianjin 300192, PR China
[b] Oriental Organ Transplant Center of Tianjin First Central Hospital, Tianjin 300192, PR China
[c] CAS Key Laboratory of Molecular Imaging, Institute of Automation, Chinese Academy of Sciences, Beijing, 100190, PR China

ARTICLE INFO

Keywords:
Artificial intelligence
Hepatocellular carcinoma
Liver transplantation
Recurrence

ABSTRACT

Objectives: To assess whether radiomics signature can identify aggressive behavior and predict recurrence of hepatocellular carcinoma (HCC) after liver transplantation.

Methods: Our study consisted of a training dataset (n = 93) and a validation dataset (40) with clinically confirmed HCC after liver transplantation from October 2011 to December 2016. Radiomics features were extracted by delineating regions-of-interest (ROIs) around the lesion in four phases of CT images. A radiomics signature was generated using the least absolute shrinkage and selection operator (LASSO) Cox regression model. The association between radiomics signature and recurrence-free survival (RFS) was assessed. Preoperative clinical characteristics potentially associated with RFS were evaluated to develop a clinical model. A combined model incorporating clinical risk factors and radiomics signature was built.

Results: The stable radiomics features associated with the recurrence of HCC were simply found in arterial phase and portal phase. The prediction model based on the radiomics features extracted from the arterial phase showed better prediction performance than the portal vein phase or the fusion signature combining both of arterial and portal vein phase. A radiomics nomogram based on combined model consisting of the radiomics signature and clinical risk factors showed good predictive performance for RFS with a C-index of 0.785 (95% confidence interval [CI]: 0.674-0.895) in the training dataset and 0.789 (95% CI: 0.620-0.957) in the validation dataset. The calibration curves showed agreement in both training (p = 0.121) and validation cohorts (p = 0.164).

Conclusions: Radiomics signature extracted from CT images may be a potential imaging biomarker for liver cancer invasion and enable accurate prediction of HCC recurrence after liver transplantation.

1. Introduction

Hepatocellular carcinoma (HCC) is the most common primary liver cancer and ranks third as a cause of cancer death worldwide [1]. In patients with an absence of clinically relevant portal hypertension, hepatectomy remains the golden standard for early stage disease [2]. However, most patients are in the middle or late stages when symptoms occur. The resection rate is less than 30%; nevertheless, the recurrence rate of 5 years is up to 70%. Liver transplantation, is the most efficient treatment for end-stage liver disease and is recommended in patients with clinically proven portal hypertension and early stage HCC meeting the Milan criteria, whereby the 5-year disease-free survival rate is up to

Abbreviations: HCC, hepatoceluller carcinoma; RFS, recurrence-free survival; MVI, microvascular invasion; CT, computed tomography; MRI, magnetic resonance imaging; RFA, radiofrequency ablation; PEI, percutaneous ethanol injection; TACE, transcatheter arterial chemoembolization; HBsAg, hepatitis B surface antigen; HCVAb, hepatitis C antibody; AFP, alpha-fetoprotein; ALT, alanineamino-transferase; GGT, γ-glutamyltranspeptadase; AST, aspartate amino-transferase; ROI, region of interest; ICC, inter- and intra-class correlation coefficients; LASSO, least absolute shrinkage and selection operator; KM, Kaplan-Meier; C-Index, concordance index; BCLC, Barcelona clinic liver cancer; MELD, model for end-stage liver disease

* Corresponding author at: Oriental Organ Transplant Center of Tianjin First Central Hospital, No. 24 Fukang Road, Nankai District, Tianjin 300192, China.
** Corresponding author at: Key Laboratory of Molecular Imaging of Chinese Academy of Sciences, Institute of Automation, Chinese Academy of Sciences, 95 Zhongguancun East Road, Beijing, 100190 China.
E-mail addresses: tian@ieee.org (J. Tian), zhenghong1965@tmu.edu.cn (H. Zheng).
[1] These authors contributed equally to this work.

https://doi.org/10.1016/j.ejrad.2019.05.010
Received 17 January 2019; Received in revised form 5 May 2019; Accepted 8 May 2019

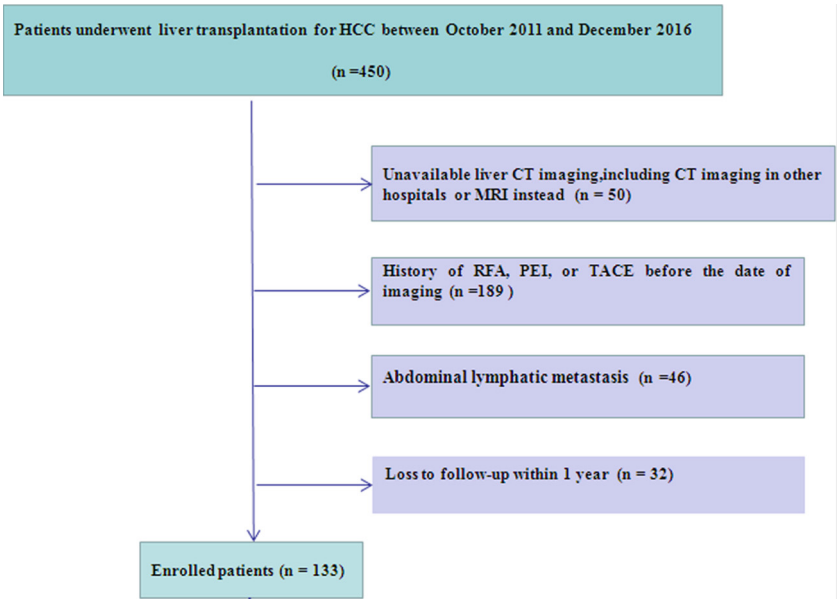

Fig. 1. Flowchart for inclusion and exclusion of patients within archive. RFA: radiofrequency ablation; PEI: percutaneous ethanol injection; TACE: transcatheter arterial chemoembolization.

60% to 80% [3,4]. The Milan criteria uses tumor size and number, but these criteria have limitations. Discordance exists between the true size and actual number of tumors seen on explant and preoperative images [5]. Microvascular invasion (MVI) and consequently, early tumor recurrence, is noted in 20% of patients undergoing liver transplantation, reducing the 5-year survival from 80% to 40% after liver transplantation [4,6,7]. Recurrence has been the main factor that affects the curative effect of HCC after liver transplantation [8]. Prospective identification of recurrence in patients with HCC thus has direct implications for organ allocation, surgical techniques, prognosis, and public policy.

Improvements in survival estimation are largely due to advances in biologic and genomic technologies that have allowed incorporation of survival-associated biologic or genetic signatures [9,10]. Previous studies have shown that risk factors such as MVI and histological differentiation of HCC are associated with recurrence after liver transplantation [4,11,12]. However, the inability to obtain comprehensive information about heterogeneous tumors remains a limitation of these invasive methods [12] Therefore, there is an urgent need for approaches that can accurately evaluate the biological characteristics of HCC preoperatively so as to predict the risk of relapse after liver transplantation.

The field of radiogenomics has recently gained interest for defining association graphs between genomic phenotypes and imaging texture features [13]. One study utilizing CT showed that 28 imaging phenotypes precisely predicted the expression information of 6,732 genes [14]. By extracting high-throughput quantitative descriptors from routine CT studies, radiogenomics could non-invasively assess tumor heterogeneity [15,16]. The high-throughput characteristics of arterial and venous phases based on quantitative imaging analysis of enhanced CT in 28 patients with hepatectomy may be potential substitute markers for MVI of HCC [17]. Previous reports have indicated that some radiomic features extracted from tumor regions of CT images, especially characteristics of arterial and portal phases, can surpass traditional indicators such as Barcelona Clinic Liver Cancer (BCLC) for assessing the efficacy of HCC hepatectomy [18]. These high-throughput characteristics related to MVI or prognosis of HCC may be potential independent predictors of HCC recurrence after liver transplantation.

Therefore, our study aimed to develop and validate a novel biomarker which could predict recurrence of HCC after liver transplantation to better stratify patients and guide organ allocation and surgical techniques.

2. Materials and methods

2.1. Ethical approval

This study was approved by the medical ethics committee of our institution. The necessity to obtain informed consent was waived.

2.2. Patients

By searching electronic medical records, 450 patients who underwent liver transplantation in our institution with histopathologically confirmed HCC were recruited. The inclusion criteria were as follows: (i) patients with HCC who underwent initial liver transplantation with curative intention between October 2011 and December 2016; (ii) those with preoperative enhancement CT in abdomen performed within 1 month; (iii) follow up for at least 1 year; (iv) no treatment was received before operation; (v) conventional anti-immune rejection (Tacrolimus Capsules, Mycophenolate Mofetil Tablets, hormone dose adjusted according to concentration) and prevention program (intraoperative administration of hepatitis B globulin 4000 IU to patients with hepatitis B, postoperative low-dose hepatitis B immunoglobulin combined with nucleoside analogues to prevent hepatitis B recurrence, and close monitoring) were obtained during and after the operation. The exclusion criteria were as follows: (i) patients with lack of available imaging data as preoperative CT was performed at some other institution (n = 24) or patients had undergone preoperative magnetic resonance imaging (MRI) instead (n = 26); (ii) those with a history of transcatheter arterial chemoembolization (TACE), percutaneous ethanol injection (PEI), or radiofrequency ablation (RFA) before the date of imaging (n = 189); (iii) those with abdominal lymphatic metastasis with pathological confirmation (n = 46); (iv) loss to follow-up within 1 year (n = 32). In total, 133 patients (114 men and 19 women; mean age, 52.52 years ± 8.17; range, 16.67–70.83 years) were enrolled in our study (Fig. 1); 51 were in line with Milan standards and 82 exceeded Milan standards. Of all patients, 42 had recurrence within 1 year after surgery, and 91 patients did not relapse. Patients were randomly assigned to the training and validation datasets at a ratio of 7:3.

2.3. Clinical characteristics

Clinical characteristics potentially related to recurrence of HCC after liver transplantation included age, gender, albumin (≤40 or > 40 g/L), total bilirubin (≤21 or > 21 umol/L), PT (≤8.8 s, 8.8–13.8 s, ≥13.8 s), Model for end-stage liver disease (MELD)score, ascites (none, mild, severe), hepatitis B surface antigen (HBsAg) or hepatitis C antibody (HCVAb) status (positive or negative), alpha-fetoprotein (AFP) (≤7 or > 7 ng/mL), alanine amino-transferase (ALT) (≤40 or > 40 U/L), γ-glutamyltranspeptadase (GGT) (≤45 or > 45 U/L), aspartate amino-transferase (AST) (≤35 or > 35 U/L), Child–Pugh grade (A, B, or C), and BCLC (A, B, C, or D). The threshold values chosen for AFP, ALT, and AST levels were based on the normal ranges used at our institution. Some patients enrolled were single hepatocellular carcinoma and some were multiple hepatocellular carcinomas in our study. Single tumor was delineated in one lesion, and the larger tumor was delineated in multiple lesions [19].

2.4. Follow-up

The end point of this study was RFS, which was defined as the time from the date of liver transplantation until the date of relapse that refers to intrahepatic recurrence or extrahepatic metastasis, or until the date that the patient was last known to be free of relapse.

All patients were continuously followed up for at least 1 year after liver transplantation until it recurred. Those without relapse were followed up to January 1, 2018. As of the last follow-up, 42 patients (31.6%) had experienced a confirmed disease relapse. The mean RFS was 969 days, and the median RFS was 852 days. The longest RFS was 2251 days, and the shortest RFS was 14 days.

Postoperative recurrence was monitored by AFP and ultrasound, or enhanced CT/MRI at the first month after operation and every 3 months thereafter. Patients with elevated AFP levels with atypical or negative imaging findings were followed up once a month or checked by biopsy. The relapse about HCC was confirmed in our research by imaging. The criteria for the diagnosis of recurrence is described in the Supplementary Information.

2.5. CT examination, region-of-interest segmentation and radiomics feature extraction

High-throughput quantitative descriptors of HCC were obtained from four phases of CT images by delineating ROI around the lesion, extracting, and analyzing radiomics features on all cross-sectional areas of the whole tumour volume in thin-layer CT images in this study. Details on image retrieval procedure, parameters for CT image scanning, tumor region segmentation, and radiomics feature extraction with reproducibility analysis are described in the Supplementary Information.

2.6. Statistical analysis

All statistical analyses were performed using SPSS (version 20) software and R platform (version 3.4.1). Mann-Whitney U test and χ^2 test were used to determine whether the values of clinical-pathologic variables were significantly different between training and validation groups. Two-sided P-values less than 0.05 were considered significantly different.

2.7. Clinical predictive model-building

Clinical characteristics with p-values < 0.05 in univariate Cox proportional hazard regression analysis were integrated into stepwise multivariate Cox proportional hazard model. Variables with p-values < 0.05 in multivariate analysis were identified as potential clinical characteristics related to survival and were included in clinical predictive model-building.

2.8. Radiomics feature selection, model-building, and evaluation

Radiomics features which had greater ICCs considering a threshold of 0.8 were robust and adopted for subsequent analysis. The LASSO method, which is appropriate for the regression of high-dimensional data [20], was utilized to select the most predictive feature set as the training dataset in Cox's proportional hazards model. For each patient, we evaluated the output of the model using a radiomics score (Rad-score) calculated by the linear combination of the selected feature set with their individual coefficients. Radiomics signature was built with the rad-score of arterial phase. A combined predictive model was built by incorporating the clinical risk factors and radiomics signature with multivariable Cox regression model. Patients were finally stratified into high-risk and low-risk groups based on the combined model with cut-off values at the median of the training dataset in arterial phase. The Log-rank test was computed to compare the two separated KM survival curves.

Performance of the clinical, radiomics, and combined models was evaluated with the concordance index (C-Index). C-Index is the area under the curve for continuous time-to-event survival data which measures the discrimination of a prognostic model. A value of 1 signifies perfect discrimination, and 0.5 represents equal discriminative power with randomness. The Hosmer-Lemeshow test was applied for the prognosis model [21]. We further built a nomogram for the model to predict the possibility of 1-year, 2-year, and 3-year RFS intuitively. Calibration curve was plotted to analyze the prognostic performance of the nomogram on both training and validation datasets [22].

3. Results

3.1. Clinical characteristics

Clinical characteristics of the training and validation datasets are shown in Table 1. A set of 93 patients and 40 patients were enrolled in training and validation cohorts respectively. Analysis of the distribution of clinical characteristics in both datasets revealed no significant differences between training and validation datasets, with p values ranging from 0.179 to 0.945 for all clinical characteristics.

All clinical characteristics were analyzed by univariate analysis and multivariate analysis in the training dataset (Table 2). After multivariate analysis, the final clinical model included HBsAg (HR (Hazard ratio, HR) = 0.255, 95% CI: 0.099-0.654; P = 0.004) and BCLC (HR = 1.373, 95% CI: 1.086–1.735); P = 0.008) as effective predictors.

3.2. Feature selection and radiomics signature building

The ROI for data extraction was evaluated in the whole volume of the tumor in four phases of CT images. However, the stable radiomics features associated with the recurrence of HCC were simply found in arterial phase and portal phase.

After the robust analysis, 84 radiomic features remained in arterial phases. Barplots for the feature stability distribution (inter- and intra-observer reproducibility) in arterial phases are presented in Fig. 2. All the selected features were adopted to the LASSO-Cox model. According to the leave-one-out cross validation, 84 stable features were reduced to nine potential predictors in arterial phase on the basis of 93 patients in the training dataset (Fig. 3). 105 stable features were reduced to one potential predictor in portal phase on the basis of 93 patients in the training dataset. The radiomics signature was established with a Rad-score calculated using the formula in Table 3. The prediction model based on the radiomics features extracted from the arterial phase showed better prediction performance than the portal vein phase or the fusion signature combining both of arterial and portal vein phase (Table 4). So the radiomics features were extracted from the arterial

Table 1
Patient characteristics in training and validation datasets.

Characteristic	Training Dataset (N = 93)	Validation Dataset (N = 40)	P value
Age, Median (IQR), year	52.497.66	51.509.36	0.522
Gender, No. (%)			0.877
Male	80 (86.0)	34 (85.0)	
Female	13 (14.0)	6 (15.0)	
Tumor diameter	4.764.11	4.072.50	0.325
MELD, Median (IQR)	15.106.63	14.807.30	0.819
Albumin, No. (%), (g/L)			0.644
≤40	71 (76.3)	32 (80.0)	
> 40	22 (23.7)	8 (20.0)	
Total bilirubin, No. (%), μmol/L			0.783
≤21	70 (75.3)	31 (77.5)	
> 21	23 (24.7)	9 (22.5)	
GGT, No. (%),45 U/L			0.705
≥45	77 (82.8)	32 (80.0)	
≤7	15 (16.1)	8 (20.0)	
7-45	1 (1.1)	0 (0)	
AST, No. (%),45 U/L			0.785
≥35	52 (55.9)	21 (52.5)	
≤13	4 (4.3)	1 (2.5)	
13-35	37 (39.8)	18 (45.0)	
ALT, No. (%),45 U/L			0.738
≤7	1 (1.1)	0 (0)	
≥40	61 (65.6)	28 (30.0)	
7-40	31 (33.3)	12 (70.0)	
PT, No. (%), s			0.682
≤13.8	55 (59.1)	25 (62.5)	
> 13.8	38 (40.9)	15 (37.5)	
AFP, No. (%), ng/mL			0.740
≤7	33 (35.5)	13 (32.5)	
> 7	60 (64.5)	27 (67.5)	
BCLC, No. (%)			0.179
A	32 (34.4)	19 (27.5)	
B	18 (19.4)	8 (17.5)	
C	8 (8.6)	0 (7.5)	
D	35 (37.6)	13 (47.5)	
Child-Pugh class, No. (%)			0.945
A	24 (25.8)	10 (25.0)	
B	39 (41.9)	18 (45.0)	
C	30 (32.3)	12 (30.0)	
Ascites, No. (%)			0.631
None	44 (47.3)	21 (52.5)	
Mild	31 (33.3)	10 (25.0)	
Severe	18 (19.4)	9 (22.5)	
HBsAg, No. (%)			0.355
Positive	70 (75.3)	27 (67.5)	
Negative	23 (24.7)	13 (32.5)	
Anti-HCV, No. (%)			0.696
Positive	19 (20.4)	7 (17.5)	
Negative	74 (79.6)	33 (82.5)	
Follow-up time, Median (IQR), month	32.625.3	32.623.3	0.934

Note: No significant differences were found between the training dataset and the validation dataset value ranged from 0. 179 to 0.945 in all the clinical factors. HBsAg, hepatitis B surface antifen; Anti − HCV, anti-hepatitis C virus antibody; AFP, alpha-fetoprotein; ALT, alanine amino-transferase; GGT, γ-glutamyltranspeptadase; AST, aspartate amino-transferase; IQR, inter-quartile range.

phase to build the predictive model finally. The patients were classified into high-risk or low-risk groups according to the combined model with cut-off value at the median of the training dataset in arterial phase. Log-rank test revealed significant differences in RFS between the high-risk and low-risk subgroups in both the training ($p < 0.001$) and validation set ($p = 0.011$) (Fig. 4).

3.3. Model performance for RFS and predictive values for RFS within or exceeding Milan standard

The C-indexes of the predictive models for RFS are shown in Table 4. The C-indexes of the clinical model for RFS in training and validation datasets were 0.675 (95% CI: 0.568–0.782) and 0.713 (95% CI: 0.549–0.877), respectively. The C-indexes of the radiomics model based on arterial phase for RFS in training and validation datasets were 0.743 (95% CI: 0.632–0.853) and 0.705 (95% CI: 0.537–0.874), respectively. The combined model with radiomics signature based on arterial phase and clinical characteristics was significantly associated with RFS in the training dataset (C-index, 0.785; 95% CI: 0.643–0.864), and this finding was confirmed in the validation dataset (C-index, 0.789; 95% CI: 0.620–0.957). It exhibited the best performance among all the models. The combined model had good predictive performance for RFS with C-index 0.773 (95% CI: 0.532–1.000) in patients within Milan standard, with C-index 0.726 (95% CI: 0.623-0.829) exceeding Milan standard (Table 5).

Table 2
Results of univariate and multi-variable analysis.

Clinical predictors	Univariate analysis		Multi-variable analysis	
	p-value	HR (95% CI)	p-value	HR (95% CI)
Gender	0.153	0.391 (0.108-1.416)		
Age	0.103	0.964 (0.922-1.007)		
MELD	0.092	1.054 (0.992-1.119)		
Albumin	0.194	0.542 (0.215-1.366)		
AFP	0.208	0.509 (0.178-1.455)		
Total bilirubin	0.526	0.699 (0.231-2.114)		
GGT	0.268	0.510 (0.155-1.681)		
AST	0.474	1.256 (0.673-2.341)		
ALT	0.990	1.006 (0.419-2.413)		
PT	0.500	1.324 (0.585-2.996)		
Ascites	0.314	1.315 (0.772-2.241)		
HBsAg	0.059	0.223 (0.047-1.059)	0.004	0.255 (0.099-0.654)
Anti-HCV	0.106	5.258 (0.704-39.251)		
Child-Pugh class	0.210	0.628 (0.304-1.299)		
BCLC	0.064	1.405 (0.981-2.014)	0.008	1.373 (1.086-1.735)
Tumor diameter	0.362	1.041 (0.955-1.134)		
Rad-score	0.004	1.893 (1.232-2.909)	< 0.001	2.287 (1.697-3.084)

Note: * P value < 0.05. HBsAg and BCLC were integrated to clinical model.

3.4. Development of an individualized prediction model

A radiomics nomogram based on the best model which included the radiomics signature in the arterial phase and efficient clinical characteristics was built (Fig. 5). Calibration curves of the nomogram for the probability of 1-year, 2-year, and 3-year RFS are shown in Fig. 6. There was an agreement between the estimation using the radiomics nomogram and actual observation, with Hosmer-Lemeshow test yielding p values of 0.121 and 0.164 in both training and validation datasets, respectively.

4. Discussion

To predict the recurrence of HCC after liver transplantation, we

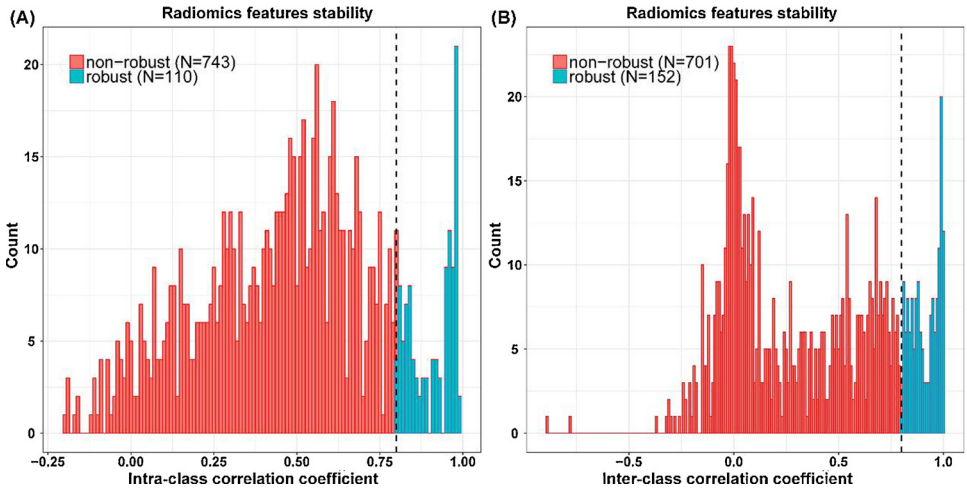

Fig. 2. Histogram of the Inter-class correlation coefficient and Intra-class correlation coefficient. After robustness test, (A) 110 and (B) 152 of the initial 853 CT image features in arterial phase were retained.

constructed a radiomics signature basing on contrast-enhanced CT images in artery phase. A multi-feature-based radiomics signature was identified to be an effective biomarker for the prediction of HCC recurrence after liver transplantation in this study, with potential prognosis value for individualized RFS. The radiomics signature successfully stratified patients with HCC into high-risk and low-risk groups, with significant differences in RFS. Furthermore, the radiomics nomogram based on the combined model which integrates effective clinical characteristics and radiomics signature showed good discrimination and prominent predictive performance for RFS in HCC patients after liver transplantation. For patients with high recurrence, liver transplantation is not recommended, so that the scarce donor liver resources can be allocated to patients who urgently need liver transplantation and have a good prognosis.

Solid tumors have spatial and temporal heterogeneity, and detection methods based on invasive biopsy have limitations that do not reflect the biological characteristics of the overall tumor, while imaging assessment has the unique ability to detect tumors as a whole, allowing observation of heterogeneity within the tumor. To a certain extent, radiomics with high dimensional features of imaging can surpass the boundaries of tumor anatomy and morphological data. In our study, radiomics was first used to predict recurrence of HCC after liver transplantation. Radiomics prediction method was established through a series of coherent comprehensive evaluations of tumor biological behavior and clinical prognosis. It is conducive to fully exploit potential images using artificial intelligence and big data technology to overcome limitations of traditional evaluation methods, improve the predictive performance of HCC recurrence after liver transplantation, facilitate the rational distribution of donors in clinical practice, and conduct necessary intraoperative or postoperative prophylactic treatment for patients with high recurrence.

Table 3
Radiomics score (Rad-score) for CT image in Arterial phase.

Phase	Radiomics signature
Arterial phase	Rad-score = 0.088 + 0.073* original_glcm_Correlation + 0.829 * original_glszm_GrayLevelNonUniformity + 0.496 * original_glszm_ZoneEntropy + 0.578 * original_shape_MajorAxis – 0.507 * wavelet.HLH_gldm_LargeDependenceEmphasis + 0.248 * wavelet.HLH_glszm_GrayLevelNonUniformity + 0.05 * wavelet.HLL_gldm_DependenceNonUniformity - 0.334 * wavelet.LHL_glrlm_RunPercentage – 0.968 * wavelet.LLL_glszm_GrayLevelNonUniformity

Note: Features were selected by LASSO modelling via leave-one cross-validation.

Our study demonstrated that nine robust radiomic features extracted form arterial phase including original_glszm_ZoneEntropy and

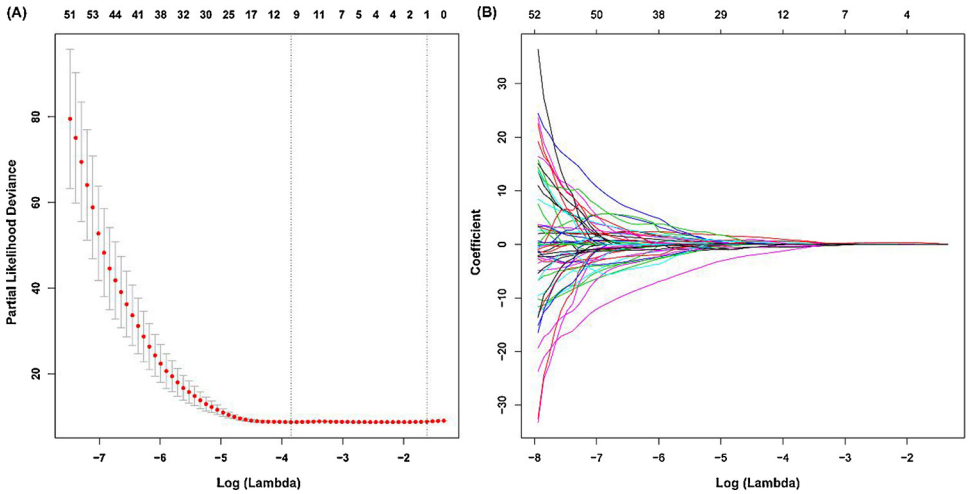

Fig. 3. Radiomics feature selection using the least absolute shrinkage and selection operator (LASSO) cox regression model. (a) Partial likelihood deviance was drawn versus log (λ) in arterial phase; (b) The coefficients of the selected features are shown by lambda parameter in arterial phase.

Table 4
Predictive performance for RFS of the proposed models.

Different models	Training Dataset N = 93 C-index (95%CI)	Validation Dataset N = 40 C-index (95%CI)
Clinical model		
Clinical factor	0.675 (0.568-0.782)	0.713 (0.549-0.877)
Radiomics model		
Arterial phase	0.743 (0.632-0.853)	0.705 (0.537-0.874)
Combined model		
Arterial phase + Clinical factor	0.785 (0.674-0.895)	0.789 (0.620-0.957)

Note. C-index (Harrell concordance index) indicates the predictive performance.

Table 5
Predictive performance for RFS of the proposed models within and exceeding Milan standard.

Different models	Within Milan standard N = 51 C-index (95%CI)	Exceeding Milan standard N = 82 C-index (95%CI)
Clinical model		
Clinical factor	0.748 (0.507-0.989)	0.639 (0.539-0.740)
Radiomics model		
Arterial phase	0.748 (0.507-0.989)	0.661 (0.559-0.764)
Combined model		
Arterial phase + Clinical factor	0.773 (0.532-1)	0.726 (0.623-0.829)

original_shape_MajorAxisetc were associated with RFS after liver transplantation. Original_shape_MajorAxis is the largest and principal component axis; it has an inverse association with elongation, which measures the degree of circle-like properties of the tumor. In our study, the less Original_shape_MajorAxis corresponded to greater elongation, which represented a rounder tumor area and better RFS [23]. The original_glszm_ZoneEntropy feature measures the uncertainty or randomness in the distribution of zone sizes and gray levels; a higher value suggests more tumor heterogeneity in texture patterns and implied worse RFS in our study. We observed that wavelet features such as wavelet_HLH_gldm_LargeDependenceEmphasis and wavelet_HLH_glszm_GrayLevelNonUniformity were associated with recurrence of HCC, consistent with previous studies [24–28].

The representations of the radiomics signature and nomogram were demonstrated to estimate RFS in our study. A recent established nomogram integrating multiple clinical-pathologic risk factors successfully estimated the overall survival for patients with resected NSCLC (Non-small-cell lung cancer, NSCLC) (C-index: 0.71) [29].Compared with long-term overall survival outcomes, RFS is an end point that avoids extended follow-up and enables earlier adjustment of therapy [30]. Thus, our study may present a more efficient tool that enables earlier personalised treatment. A combined model incorporating clinical risk factor and radiomics signature had the most optimal performance of the three predictive models, which is consistent with previous results [31]. Radiomics analyses were performed on the whole tumor rather than the maximum cross section area in our study. One study showed better separation of entropy and uniformity in whole tumor analysis compared to the maximum cross section area for 5-year overall survival [32].

China has the highest incidence of liver cancer in the world. Many patients with HCC are eager to undergo liver transplantation every year. The Milan standard has limitations and does not comprehensively assess the biological characteristics, aggressive behavior, and RFS of HCC. The radiomics model we have established can more comprehensively evaluate tumor biological characteristics of HCC, and it can be used as a supplement to the Milan standard in selecting liver transplant patients.

There are several limitations in our study. First, this study was retrospective with unavoidable potential bias. Reproducibility and variability of radiomics research can be influenced by slice thickness and machine acquisition parameters [24,33] Nevertheless, we carefully selected patients who underwent abdomen enhancement CT scans with sheet thicknesses of 1.25 mm and removed patients who had received treatment before the operation. This may have excluded any patients, but minimized bias of radiomics features. Despite these limiting factors, our study highlights the potential predictive value for CT-based radiomics signature as a prognostic marker for liver cancer patients after liver transplantation. Although the usefulness of the proposed nomogram lacks external validation, calibration curve analysis demonstrated that the radiomics nomogram was consistent with actual observations for the probability of tumor recurrence at 1, 2, or 3 years. This indicates that radiomics signature has the potential to be used as a biomarker for recurrence in HCC patients after liver transplantation. Further, radiomics can be used to predict MVI and histopathological differentiation closely related to prognosis of HCC.Radiomics technique is expected to become an important cornerstone of accurate diagnosis and treatment of HCC.

5. Conclusion

Our study indicates that radiomics signature has the potential to be used as a biomarker for recurrence in HCC patients after liver

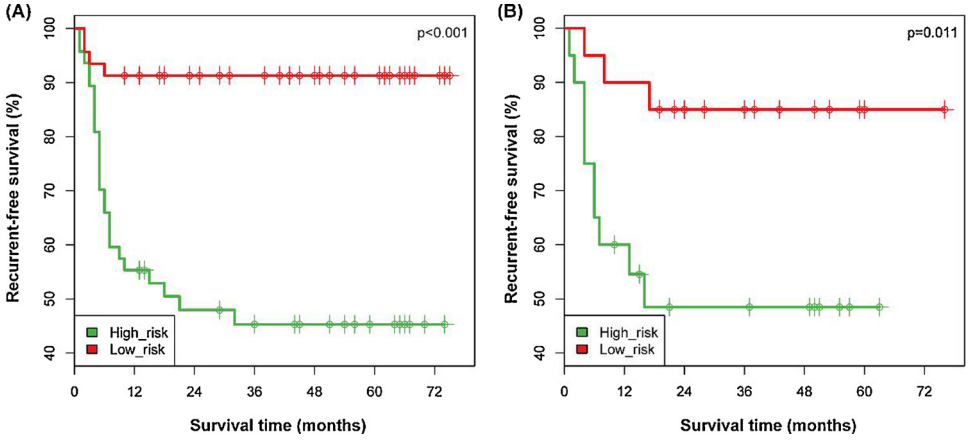

Fig. 4. Kaplan-Meier analysis in the (A) training dataset and (B) validation dataset of recurrent free survival based on the combined model with cut-off value at the median of the training dataset in arterial phase.

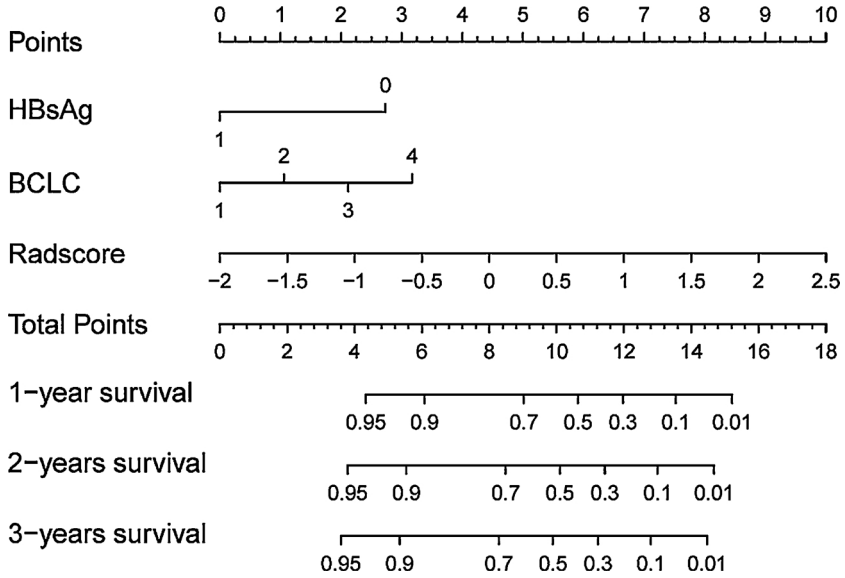

Fig. 5. The nomogram obtained from the model constructed by arterial phase radiomics signature.

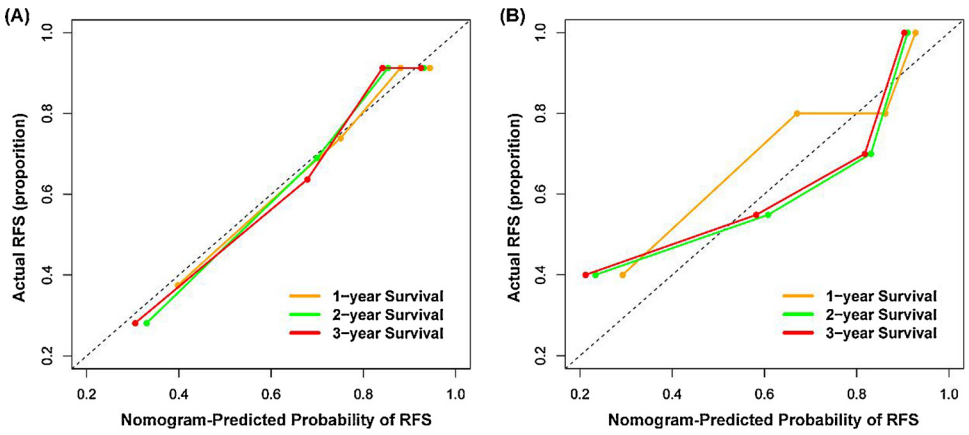

Fig. 6. Calibration curves of the radiomics nomogram in (a) training dataset and (b) validation dataset. The y-axis represents the actual RFS rate, the x-axis represents the predicted RFS possibility, and the diagonal dashed line indicates the ideal prediction by a perfect model.

transplantation, and may predict recurrence of HCC after liver transplantation as well as guide organ allocation and surgical technique in clinical practice.

Conflict of interest

None.

Grants and financial support

This paper is supported by National Natural Science Foundation of China (No. 81227901, 81527805, 61231004, 81771924, 81501616), National Key R&D Program of China (2017YFA0205200, 2017YFC1308700), the Science and Technology Service Network Initiative of the Chinese Academy of Sciences (KFJ-SW-STS-160), Tianjin Clinical Research Center for Organ Transplantation Project (No. 15ZXLCSY00070).

Author contributions

The conception and design of the study, or acquisition of data, or analysis and interpretation of data: DG DG HW JW ZW QJ HZ.

Drafting the article or revising it critically for important intellectual content: DG DG HW JW ZW XH QJ SC ZS JJ ZS.

Appendix A. Supplementary data

Supplementary material related to this article can be found, in the online version, at doi:https://doi.org/10.1016/j.ejrad.2019.05.010.

References

[1] J. Ding, H. Wang, Multiple interactive factors in hepatocarcinogenesis, Cancer Lett. 346 (2014) 17–23.
[2] M.E. Akoad, E.A. Pomfret, Surgical resection and liver transplantation for hepatocellular carcinoma, Clin. Liver Dis. 19 (2015) 381–399.
[3] Y. Fong, R.L. Sun, W. Jarnagin, L.H. Blumgart, An analysis of 412 cases of hepatocellular carcinoma at a Western center, Ann. Surg. 229 (790-799) (1999) 799–800.
[4] K.C. Lim, P.K. Chow, J.C. Allen, et al., Microvascular invasion is a better predictor of tumor recurrence and overall survival following surgical resection for hepatocellular carcinoma compared to the Milan criteria, Ann. Surg. 254 (2011) 108–113.
[5] M.S. Reddy, D.M. Manas, Accuracy of staging as a predictor for recurrence after liver transplantation for hepatocellular carcinoma, Transplantation 83 (2007) 367–368.
[6] M. Renzulli, F. Buonfiglioli, F. Conti, et al., Imaging features of microvascular invasion in hepatocellular carcinoma developed after direct-acting antiviral therapy in HCV-related cirrhosis, Eur. Radiol. 28 (2018) 506–513.
[7] M.J. Kim, M. Lee, J.Y. Choi, Y.N. Park, Imaging features of small hepatocellular carcinomas with microvascular invasion on gadoxetic acid-enhanced MR imaging, Eur. J. Radiol. 81 (2012) 2507–2512.
[8] A. Taketomi, T. Fukuhara, K. Morita, et al., Improved results of a surgical resection for the recurrence of hepatocellular carcinoma after living donor liver transplantation, Ann. Surg. Oncol. 17 (2010) 2283–2289.

[9] S. Halabi, C.Y. Lin, W.K. Kelly, et al., Updated prognostic model for predicting overall survival in first-line chemotherapy for patients with metastatic castration-resistant prostate cancer, J. Clin. Oncol. 32 (2014) 671–677.
[10] J.X. Zhang, W. Song, Z.H. Chen, et al., Prognostic and predictive value of a microRNA signature in stage II colon cancer: a microRNA expression analysis, Lancet Oncol. 14 (2013) 1295–1306.
[11] V. Mazzaferro, J.M. Llovet, R. Miceli, et al., Predicting survival after liver transplantation in patients with hepatocellular carcinoma beyond the Milan criteria: a retrospective, exploratory analysis, Lancet Oncol. 10 (2009) 35–43.
[12] K.M. Chan, H.S. Chou, T.J. Wu, C.F. Lee, Lee W.C. Yu MC, Characterization of hepatocellular carcinoma recurrence after liver transplantation: perioperative prognostic factors, patterns, and outcome, Asian J. Surg. 34 (2011) 128–134.
[13] V. Hofman, M. Ilie, E. Long, et al., Immunohistochemistry and personalised medicine in lung oncology: advantages and limitations, Bull. Cancer 101 (2014) 958–965.
[14] M.D. Kuo, N. Jamshidi, Behind the numbers: decoding molecular phenotypes with radiogenomics–guiding principles and technical considerations, Radiology 270 (2014) 320–325.
[15] P. Lambin, E. Rios-Velazquez, R. Leijenaar, et al., Radiomics: extracting more information from medical images using advanced feature analysis, Eur. J. Cancer 48 (2012) 441–446.
[16] H.J. Aerts, E.R. Velazquez, R.T. Leijenaar, et al., Decoding tumour phenotype by noninvasive imaging using a quantitative radiomics approach, Nat. Commun. 5 (2014) 4006.
[17] S. Bakr, S. Echegaray, R. Shah, et al., Noninvasive radiomics signature based on quantitative analysis of computed tomography images as a surrogate for microvascular invasion in hepatocellular carcinoma: a pilot study, J. Med. Imaging Bellingham (Bellingham) 4 (2017) 41303.
[18] S. Chen, Y. Zhu, Z. Liu, C. Liang, Texture analysis of baseline multiphasic hepatic computed tomography images for the prognosis of single hepatocellular carcinoma after hepatectomy: a retrospective pilot study, Eur. J. Radiol. 90 (2017) 198–204.
[19] L. Yang, D. Dong, M. Fang, et al., Can CT-based radiomics signature predict KRAS/NRAS/BRAF mutations in colorectal cancer? Eur. Radiol. 28 (5) (2018) 2058–2067.
[20] W. Sauerbrei, P. Royston, H. Binder, Selection of important variables and determination of functional form for continuous predictors in multivariable model building, Stat. Med. 26 (30) (2007) 5512–5528.
[21] D.W. Hosmer Jr, S. Lemeshow, R.X. Sturdivant, Applied Logistic Regression, John Wiley & Sons, 2013.
[22] V.P. Balachandran, M. Gonen, J.J. Smith, R.P. DeMatteo, Nomograms in oncology: more than meets the eye, Lancet Oncol. 16 (4) (2015) e173–e180.
[23] T.H. Wu, E. Hatano, K. Yamanaka, et al., A non-smooth tumor margin on preoperative imaging predicts microvascular invasion of hepatocellular carcinoma, Surg. Today 46 (2016) 1275–1281.
[24] K.A. Miles, B. Ganeshan, M.R. Griffiths, R.C. Young, C.R. Chatwin, Colorectal cancer: texture analysis of portal phase hepatic CT images as a potential marker of survival, Radiology 250 (2009) 444–452.
[25] F. Ng, B. Ganeshan, R. Kozarski, K.A. Miles, V. Goh, Assessment of primary colorectal cancer heterogeneity by using whole-tumor texture analysis: contrast-enhanced CT texture as a biomarker of 5-year survival, Radiology 266 (2013) 177–184.
[26] V. Goh, B. Ganeshan, P. Nathan, J.K. Juttla, A. Vinayan, K.A. Miles, Assessment of response to tyrosine kinase inhibitors in metastatic renal cell cancer: CT texture as a predictive biomarker, Radiology 261 (2011) 165–171.
[27] H. Zhang, C.M. Graham, O. Elci, et al., Locally advanced squamous cell carcinoma of the head and neck: CT texture and histogram analysis allow independent prediction of overall survival in patients treated with induction chemotherapy, Radiology 269 (2013) 801–809.
[28] B. Ganeshan, E. Panayiotou, K. Burnand, S. Dizdarevic, K. Miles, Tumour heterogeneity in non-small cell lung carcinoma assessed by CT texture analysis: a potential marker of survival, Eur. Radiol. 22 (2012) 796–802.
[29] W. Liang, L. Zhang, G. Jiang, et al., Development and validation of a nomogram for predicting survival in patients with resected non-small-cell lung cancer, J. Clin. Oncol. 33 (2015) 861–869.
[30] A. Mauguen, J.P. Pignon, S. Burdett, et al., Surrogate endpoints for overall survival in chemotherapy and radiotherapy trials in operable and locally advanced lung cancer: a re-analysis of meta-analyses of individual patients' data, Lancet Oncol. 14 (2013) 619–626.
[31] Y. Zhou, L. He, Y. Huang, S. Chen, P. Wu, W. Ye, et al., CT-based radiomics signature: a potential biomarker for preoperative prediction of early recurrence in hepatocellular carcinoma, Abdom. Radiol. 42 (6) (2017) 1695–1704.
[32] F. Ng, R. Kozarski, B. Ganeshan, V. Goh, Assessment of tumor heterogeneity by CT texture analysis: can the largest cross-sectional area be used as an alternative to whole tumor analysis? Eur. J. Radiol. 82 (2) (2013) 342–348.
[33] P. Guggenbuhl, D. Chappard, M. Garreau, J.Y. Bansard, G. Chales, Y. Rolland, Reproducibility of CT-based bone texture parameters of cancellous calf bone samples: influence of slice thickness, Eur. J. Radiol. 67 (2008) 514–520.